Journal of Neurochemistry, 2004, **91**, 778–787 doi:10.1111/j.1471-4159.2004.02716.x

Dynamic or inert metabolism? Turnover of *N*-acetyl aspartate and glutathione from D-[1-^{13}C]glucose in the rat brain *in vivo*

In-Young Choi* and Rolf Gruetter†

**The Nathan Kline Institute, Medical Physics, Orangeburg, New York, USA*

†*Center for Magnetic Resonance Research, Department of Radiology and Neuroscience, University of Minnesota Medical School, Minneapolis, Minnesota, USA*

Abstract

The rate of ^{13}C-label incorporation into both aspartyl (NAA C3) and acetyl (NAA C6) groups of *N*-acetyl aspartate (NAA) was simultaneously measured in the rat brain *in vivo* for up to 19 h of [1-^{13}C]glucose infusion ($n = 8$). Label incorporation was detected in NAA C6 approximately 1.5 h earlier than in NAA C3 because of the delayed labeling of the precursor of NAA C3, aspartate, compared to that of NAA C6, glucose. The time courses of NAA were fitted using a mathematical model assuming synthesis of NAA in one kinetic compartment with the respective precursor pools of aspartate and acetyl coenzyme A (acetyl-CoA). The turnover rates of NAA C6 and C3 were 0.7 ± 0.1 and 0.6 ± 0.1 μmol/(g h) with the time constants 14 ± 2 and 13 ± 2 h, respectively, with an estimated pool size of 8 μmol/g. The results suggest that complete label turnover of NAA from glucose occurs in approximately 70 h. Several hours after starting the glucose infusion, label incorporation into glutathione (GSH) was also detected. The turnover rate of GSH was 0.06 ± 0.02 μmol/(g h) with a time constant of 13 ± 2 h. The estimated pool size of GSH was 0.8 μmol/g, comparable to the cortical glutathione concentration. We conclude that NAA and GSH are completely turned over and that the metabolism is extremely slow (< 0.05% of the glucose metabolic rate).

Keywords: brain, glutathione, *in vivo*, metabolism, *N*-acetyl aspartatem, nuclear magnetic resonance.

J. Neurochem. (2004) **91,** 778–787.

The measurement of a neurochemical turnover using ^{13}C as a 'tracer' has provided an opportunity to explore metabolic fluxes and an important parameter to study brain energy metabolism (Cerdan *et al*. 1990; Bachelard and Badar-Goffer 1993; Gruetter 2002). Using *in vivo* ^{13}C NMR, the metabolic rate of neurochemicals can be assessed by measuring the rate of label incorporation from the ^{13}C-labeled precursor into metabolites, including amino acids. When considering metabolic steady state (i.e. metabolite concentrations and flux rates are assumed constant in time), a rapid rise in isotopic enrichment of the precursor results in labeling of metabolites, which is in general slower than that of the precursor. The labeling turnover time is related to the label half-life, the pool size and the turnover (or metabolic) rate assuming concentration changes of metabolites are small at steady state (for details see Choi and Gruetter 2003; Gruetter 2004). Therefore, label incorporation into various neurochemicals occurs on a distinctively different time scale. For example, label incorporation into glucose, glutamate/glutamine and glycogen occurs with a label half-life, $T_{1/2}$ ($T_{1/2}$ is typically defined as the time it takes to replace half the ^{12}C with ^{13}C and vice versa, following a step change in precursor enrichment), on the order of ~10 min, 1–2 h and > 10 h, respectively (Hyder *et al*. 1996; Choi and Gruetter 2000, 2003). Although the label turnover of major amino acids from [^{13}C]glucose, such as glutamate and glutamine, has been well studied and reported to be relatively fast (Rothman *et al*. 1999; Gruetter 2002), that of *N*-acetyl aspartate (NAA) and glutathione (GSH) has been rarely measured *in vivo* and is considered to be very slow or maybe inert (Clarke *et al*.

Received May 7, 2003; revised manuscript received June 15, 2004; accepted June 16, 2004.

Address correspondence and reprint requests to In-Young Choi, The Nathan Kline Institute, 140 Old Orangeburg Road, Bldg 35, Orangeburg, NY 10962, USA. E-mail: iychoi@nki.rfmh.org

Abbreviations used: acetyl-CoA, acetyl coenzyme A; Glu, glutamate; GSH, glutathione; NAA, *N*-acetyl aspartate; NAAG, *N*-acetyl aspartyl glutamate; NOE, nuclear Overhauser effect; RF, radiofrequency; TCA, cycle, tricarboxylic acid cycle; TR, repetition time; VOI, volume of interest.

1975; Kunnecke *et al*. 1993; Chang *et al*. 1997; Gruetter *et al*. 1998b; Tyson and Sutherland 1998; Moreno *et al*. 2001). Therefore, we sought to measure the turnover rate of two slow metabolites, NAA and GSH.

NAA is the most abundant amino acid in the adult brain, reaching concentrations on the order of 10 μmol/g, and is of increasing importance in medical diagnostics. NAA is localized to neurons (Nadler and Cooper 1972) and undergoes dramatic increases during brain development in all regions of the rat brain (Tallan 1957; Tkac *et al*. 2003), suggesting important, as of yet unknown roles in brain function (for reviews, see Clark 1998; Baslow 2003). Even though its precise function in the central nervous system remains elusive, NAA has been recognized as a putative neuronal marker, possibly reflecting neuronal cell volume (Meyerhoff *et al*. 1993). However, this role assumes that there is little or no active NAA metabolism that might alter its concentration. The biosynthesis of NAA occurs in the neuro-axonal compartment from its precursors, aspartate and acetyl coenzyme A (acetyl-CoA), through the action of the enzyme, L-aspartate-*N*-acetyltransferase, or from *N*-acetyl aspartyl glutamate (NAAG) by N-acetylated α-linked amino dipeptidase (Tyson and Sutherland 1998). NAA is then transported from the mitochondrion to the cytoplasm, and metabolized by *N*-acetylaspartate amidohydrolase (or aspartoacylase) to yield aspartate and acetate, and releasing amino nitrogen and carbon in the cytosol. Many functions have been proposed for NAA, including osmoregulation (Taylor *et al*. 1995; Baslow 2000) or as a precursor of acetate. It may also be a breakdown product of the neurotransmitter NAAG (Blakely and Coyle 1988). Another proposed role of NAA may be a facet of a storage form of aspartate, acetyl-CoA, and acetyl groups for myelin synthesis (D'Adamo *et al*. 1968). Lastly, NAA has also been proposed to serve as a mitochondrial shuttle of acetyl-CoA used for fatty acid synthesis (D'Adamo and Yatsu 1966).

It is accepted that NAA metabolism is very slow compared to the cerebral metabolic rates of glucose and oxygen (Tyson and Sutherland 1998). Nonetheless, a quantitative assessment of NAA metabolism may provide important insight into the neuronal and mitochondrial integrity of the brain in health and various neurological disorders. The endogenous NAA pool was thought to be virtually metabolically inert because of its slow label incorporation after the administration of ^{14}C- or ^{13}C-labeled precursors (Jacobson 1959; Margolis *et al*. 1960; O'Neal *et al*. 1966). However, using tissue extraction, a few studies have suggested a slow turnover rate of NAA in the rat brain (Clarke *et al*. 1975; Kunnecke *et al*. 1993; Tyson and Sutherland 1998). Interestingly a recent report by Moreno *et al*. (2001) showed label incorporation from glucose into NAA C2 only, although label incorporation into all three resonances of NAA is expected, as demonstrated in our preliminary work (Choi and Gruetter 2000).

In addition to NAA, another important molecule, GSH can be measured *in vivo* in the brain using ^{13}C NMR (Choi *et al*. 2000). However, to date, the turnover of GSH has not been demonstrated in the intact living brain *in vivo*, possibly because of its slow metabolism. GSH, a sensitive indicator of oxidative stress, plays a major role in the protection against reactive oxygen species (Ketterer 1988; Coyle and Puttfarcken 1993) and in the regulation of redox status (Ogita *et al*. 1995; Varga *et al*. 1997). In addition to its critical role as an antioxidant, GSH may serve as a regulator of signal transduction for long-term potentiation or apoptosis, may protect against the excitotoxic effects of glutamatergic action (Coyle and Puttfarcken 1993), and possibly is itself a neurotransmitter (Guo *et al*. 1992; Shaw *et al*. 1996). Experimental evidence suggests a close relationship between the decrease of GSH and neural degeneration in animal (Benzi *et al*. 1988) and human studies (Lang *et al*. 1992). GSH is not only related to several neurodegenerative diseases but is also essential for normal brain function (Bains and Shaw 1997; Dringen *et al*. 1999).

The biosynthesis of GSH occurs from its precursors, glycine and γ-glutamylcysteine, through the action of the enzyme, GSH synthetase. γ-Glutamylcysteine is formed from cysteine and glutamate by the enzyme, γ-glutamyl synthetase, which is normally the rate-limiting enzyme in GSH synthesis (Chang *et al*. 1997). The biosynthesis of GSH is also catalyzed by glutathione reductase, which uses NADPH + H^+ produced by the pentose phosphate pathway. GSH has been measured using NMR in cells (Brown *et al*. 1977; Kuchel and Chapman 1983; Jans and Leibfritz 1988; Skibsted and Hansen 1990; Dringen *et al*. 1998) and in other organs (Farnsworth and Schleich 1985; Cohen 1987). In the brain, an increase in GSH synthetase activity during oxidative stress has been reported and GSH turnover was determined in mice (Chang *et al*. 1997). Using *in vivo* ^{13}C NMR, cerebral GSH metabolism can be measured from the label incorporation from ^{13}C-labeled glucose into GSH (Choi *et al*. 2000), and the turnover of GSH can be determined non-invasively from a single animal. Following infusion of [1-^{13}C]glucose, the methylene group of γ-glutamylcysteine is labeled from the C4 methylene carbon of glutamate (Glu C4), which is the label precursor of the C4 methylene carbon of the glutamyl group of GSH (GSH Glu C4).

In this study, we employed three-dimensionally localized *in vivo* ^{13}C NMR spectroscopy to detect ^{13}C-label incorporation into NAA and GSH from ^{13}C-labeled glucose. The aim of the present study was (i) to measure *in vivo* metabolism, turnover rates and compartmentation of NAA, a putative neuronal marker, and (ii) to determine *in vivo* metabolism and the turnover rate of GSH, an important antioxidant, in the rat brain. A preliminary account of part of this work has been published (Choi and Gruetter 2000).

Materials and methods

Animal preparation

The study was performed according to the guidelines for the care and use of laboratory animals at the University of Minnesota and was approved by the Institutional Animal Care and Use Committee (IACUC). Eight male Sprague-Dawley rats (265 ± 26 g, mean ± SD) were fasted overnight (over 12 h) with free access to water before studies. For preparation, animals were anesthetized with 2% isoflurane (Marsam Pharmaceuticals, Cherry Hill, NJ, USA) in a 1:1 mixture of nitrous oxide (N_2O) and oxygen (O_2), intubated, and ventilated with a pressure-driven ventilator (Kent Scientific, Litchfield, CT, USA). Then catheters were inserted both into femoral arteries and into veins. The arterial lines were used for blood gas analyses and continuous monitoring of arterial blood pressure. Arterial blood was sampled through a Teflon tubing line (Spectrum Chromatography, Houston, TX, USA) for blood gas analysis and glucose measurements at approximately 25-min intervals. The venous lines were used for intravenous infusion of α-chloralose and glucose. End-tidal CO_2 was continuously monitored with a capnometer (SC-300, BCI International, Waukesha, WI, USA). A multitrace recorder (AcqKnowledge, Biopak Co., Santa Barbara, CA, USA) was used for continuous recording of arterial blood pressure and respiratory pressure pattern. Body temperature was maintained at 37.0 ± 0.5°C with a warm-water circulation system based on feedback obtained from a rectal thermosensor (Cole Palmer, Vernon Hills, IL, USA). After securing vascular access, anesthesia was switched to α-chloralose with a bolus continuous infusion [initial bolus of 40 mg/kg followed by a continuous i.v. infusion of 24–26.7 mg/(kg h)], as described previously (Choi *et al*. 1999, 2001). The animals were secured using an in-house-built Delrin holder with a bite bar and two ear inserts to provide a three-point stereotaxic fixation of the skull to minimize motion. The animal was then placed in an acrylic holder attached to an insert placed inside the gradient coil. A 20% weight/volume solution of 99%-enriched D-[1-^{13}C]glucose (Isotec Inc., Miamisburg, OH, USA and Cambridge Isotope Laboratories, Andover, MA, USA) was infused into the left femoral vein according to the protocol used in our previous studies (Choi *et al*. 1999, 2001, 2002, 2003). In brief, the infusion rate of glucose was adjusted continuously throughout the experiment based on the NMR signal of brain glucose and concomitantly measured plasma glucose concentrations.

NMR methods

All experiments were performed on a 9.4 T, 31-cm horizontal-bore magnet (Magnex Scientific, Abingdon, UK), interfaced to an INOVA console (Varian, Palo Alto, CA, USA). An actively shielded gradient coil with an 11-cm inner diameter (Magnex Scientific) capable of switching to 300 mT/m in 500 μs was used. A quadrature polarized ^{1}H surface radiofrequency (RF) coil (14-mm diameter) combined with a linearly polarized three-turn ^{13}C RF coil (12-mm diameter) was used as a transceiver for ^{1}H NMR and ^{13}C NMR (Adriany and Gruetter 1997) and placed on the animal's head (Choi *et al*. 2001). A 99% ^{13}C-enriched formic acid sphere placed at the center of the ^{13}C coil was used as an external reference (Choi *et al*. 1999). Automated localized shimming using a fully adiabatic version of FASTMAP (Gruetter 1993) was used to adjust the currents in all first- and second-order shim coils, which were capable of generating shim fields of up to 80 Hz/(cm^2 A). The shim power supply generated up to 4 A of current at maximal voltage of 24 V (Resonance Research Incorporated, Billerica, MA, USA). Shimming resulted in a full width at half-maximum of approximately 20 Hz of the *in vivo* water signal in a nominal ∼500 μL volume ($8.5 \times 6 \times 10$ mm^3). Three-dimensional localization of the ^{13}C NMR signals based on outer volume suppression (Choi *et al*. 2000) was applied to select a volume of interest (VOI). The VOI was placed in the rat brain to avoid signal contamination from extracerebral tissues such as adipose tissue and muscle, and the VOI contained mostly cortical gray matter, given the sensitive profile of the RF coil and the small amount (8%) of white matter in the rat brain (Choi *et al*. 1999, 2000, 2002). Data were acquired with a repetition time (TR) of 1.5 s and an acquisition time of 150 ms. During these times, bi-level WALTZ-16 decoupling was applied to the proton channel for NOE (nuclear Overhauser effect) generation between excitations and for decoupling during the acquisition time.

Spectral analysis was performed using the peak-fitting algorithm supplied by the spectrometer software. To reduce variability of peak-fitting, peak linewidths of ^{13}C–^{13}C doublets were set to that of the corresponding center peak and the frequencies of the ^{13}C–^{13}C doublets were set relative to the main resonance in spectra based on their relative position determined in spectra summed for 1 h at isotopic steady state. Concentrations of ^{13}C label of NAA and GSH were calculated from the area of the fitted peaks, including the doublets for NAA. The residual was visually inspected to verify proper convergence of the peak fitting routine.

The ^{13}C-labeled NAA and GSH resonances were quantified using the external reference method, as described previously (Choi *et al*. 1999). In short, *in vivo* ^{13}C NMR signals were quantified by comparison with the measurements of solutions containing 500 mM NAA and 100 mM GSH. The external reference measurements were performed under identical experimental conditions as *in vivo*. The corrections of coil loading effect on sensitivity were assessed by measuring the pulse duration of 180° for a square pulse applied on-resonance to the signals of the ^{13}C formic acid, which was placed at the center of the ^{13}C coil. The NOE and longitudinal relaxation time (T_1) effects were corrected by measuring the saturation factors from the ^{13}C signals with a TR of 7.5 s without NOE generation, which is more than fivefold longer than the T_1 of metabolites (Choi *et al*. 2000). The excitation profile of the RF pulse, an adiabatic half-passage pulse (pulse duration of 500 μs), led to ∼28% reduction of the sensitivity at the chemical shift of NAA C2 region compared to the on-resonance sensitivity, in addition to the increased chemical shift displacement error at the NAA C2 region. The effect of limited off-resonance excitation of the adiabatic RF pulse on quantification of ^{13}C concentrations was inherently taken into account by the external reference quantification method.

NAA metabolism and modeling

The metabolic scheme of NAA metabolism is depicted in Fig. 1. Following infusion of [1-^{13}C]glucose, the C2 methyl carbon of acetyl-CoA (acetyl-CoA C2) is rapidly labeled. This is the label precursor of the C6 methyl carbon of the acetyl group of NAA (NAA C6). The label in acetyl-CoA C2 enters the tricarboxylic acid (TCA) cycle, where it is exchanged between the mitochondrial TCA cycle intermediates and the large cytosolic amino acid pools, such as glutamate C4 (Glu C4). The label continues through the TCA cycle

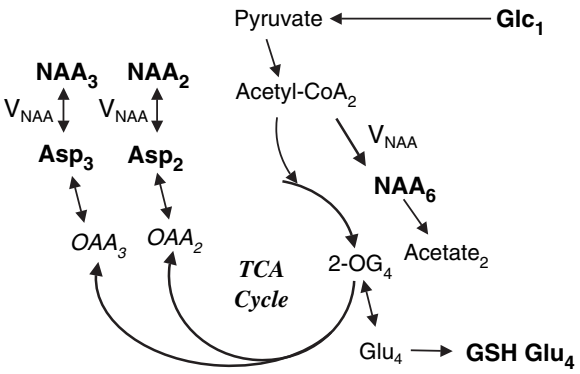

Fig. 1 Scheme of synthesis of *N*-acetyl aspartate (NAA) from glucose. In this scheme, glucose labeled at the C1 position (Glc_1) leads to labeling of the C2 methyl carbon of acetyl-CoA (acetyl-CoA_2) as a result of glucose metabolism. The label then passes into the C6 position of NAA (NAA_6) and the C2 and C3 positions of NAA (NAA_2 and NAA_3) after scrambling in the tricarboxylic acid (TCA) cycle, where it exchanges label with the large amino acid pools such as glutamate (Glu_4). Labeling of aspartate C2 (Asp_2) and C3 (Asp_3) is influenced by this exchange and is the precursor for labeling of the aspartyl moiety of NAA. 2-OG, 2-oxoglutarate; OAA, oxaloacetate; GSH Glu_4, the C4 methylene carbon of the glutamyl group of GSH.

and scrambles at succinate, a symmetric molecule. Successive label incorporation into oxaloacetate results in the symmetric labeling of the C2 methyne and C3 methylene carbons of aspartate (aspartate C2 and C3) due to exchange with oxaloacetate, both of which are the label precursors of the C2 methyne and C3 methylene carbons of the aspartyl group of NAA (NAA C2 and C3). Therefore, as a result of simultaneous synthesis and degradation of NAA, label incorporation into acetyl-CoA and aspartate from glucose is expected to result in labeling of the NAA C6 and NAA C2, C3, respectively.

Metabolism of NAA C3 and C6 was modeled based on the scheme in Fig. 1 using the following expressions (see Appendix for derivation).

$$\frac{^{13}NAA_6(t)}{NAA} = 0.5 - 0.489e^{\left(\frac{-t}{\tau_{NAA}}\right)} \quad (1)$$

$$\frac{^{13}NAA_3(t)}{NAA} = 0.5 - 0.489\left(1 + \frac{V_{NAA}}{NAA}\frac{\tau_{NAA}\tau_{Asp}}{\tau_{NAA} - \tau_{Asp}}\right)e^{\left(\frac{-t}{\tau_{NAA}}\right)} + 0.489\frac{V_{NAA}}{NAA}\frac{\tau_{NAA}\tau_{Asp}}{\tau_{NAA} - \tau_{Asp}}e^{\left(\frac{-t}{\tau_{Asp}}\right)} \quad (2)$$

The concentration and the metabolic rates of NAA were assumed to be in steady state with no net synthesis or degradation. It was further assumed that the isotopic enrichment of acetyl-CoA, the precursor of NAA C6, reaches steady state immediately compared to that of NAA. The turnover rate of NAA C6 was calculated using eqn 1. The isotopic enrichment of aspartate, the precursor of NAA C3, does not reach steady state immediately; instead it is delayed by the label exchange between intermediary metabolites in the mitochondrion and the cytosolic amino acids. The turnover rate of NAA C3 was calculated using a two-exponential fit reflecting the delayed labeling of aspartate expressed in an exponential input function (eqn 2). The time constants for NAA (τ_{NAA}) and GSH (τ_{GSH}) turnover were determined from the fitting of the time courses of NAA and GSH. The label half-life of NAA ($T_{1/2\ NAA}$) and that of GSH ($T_{1/2\ GSH}$) were defined as $\ln 2 \cdot \tau_{NAA}$ and $\ln 2 \cdot \tau_{GSH}$, respectively.

In addition to the mathematical modeling (see above and Appendix), isotopomer analysis of aspartate C3 and NAA C3 was performed to characterize the pattern of label incorporation, which provided additional information on the precursor–product relationship between aspartate and NAA. The isotopomer analysis consisted of signal integration of doublet and singlet signals of aspartate C3 and NAA C3 resonances, respectively. Singlet represents single labeling of the C3 position of aspartate and NAA without respective labeling of the C2 position, whereas doublet represents double labeling of aspartate and NAA in both C2 and C3 positions, where the resonance is split by homonuclear ^{13}C–^{13}C J coupling. Thus, the labeling ratio of doublet-to-(doublet + singlet) reflects the fraction of simultaneous ^{13}C labeling of C2 and C3 positions compared to that of the C3 position.

Results

^{13}C-label incorporation into the carbons of both the aspartyl and acetyl groups of NAA was detected during [1-^{13}C]glucose infusion (Fig. 2a). The signal intensity of all three ^{13}C NMR resonances of NAA C3 (40.5 ppm), NAA C6 (22.8 ppm) and NAA C2 (54.0 ppm) clearly increased progressively with time (Fig. 2a, 1024 scans each, TR = 1.5 s). It was interesting to note that the resonance of NAA C6 (the acetyl moiety) appeared faster than that of NAA C2 and C3 (the aspartyl moieties), as shown in the time courses (Fig. 3a). An expansion of the first 4 h at higher temporal resolution made the delay even more apparent (Fig. 3b). Close inspection of the spectral region at 40.5 ppm containing the resonance of NAA C3 featured several additional apparent resonances (Fig. 2b, top trace). Although the GABA C4 resonance at 40.4 ppm was expected to contribute to that spectral region, additional resonances were observed that were attributed to the ^{13}C–^{13}C homonuclear coupling within NAA C3 and GABA C4. This assessment was further supported by peak fitting that indicated a separation of 34 Hz of these small resonances about their respective chemical shift of both metabolites, consistent with the ^{13}C–^{13}C J coupling constant typically seen for amino acids (Henry *et al*. 2003). Therefore, the resonances around the NAA C3 at 40.5 ppm can be described as a combination of singly labeled (singlet) and doubly labeled (doublet) NAA C3, and singlet and doublet of GABA C4 signals (Fig. 2b, bottom trace). The faster appearance of the resonances of GABA C4 compared to that of NAA C3 was consistent with the faster GABA metabolism compared to that of NAA in the brain *in vivo*.

The time course of NAA C6 was fitted using eqn 1 and the estimated turnover rate of NAA C6 was $V_{NAA} = 0.7 \pm 0.1$ μmol/(g h) with the time constant of NAA C6 from the turnover fit, $\tau_{NAA6} = 14 \pm 2$ h (mean ± SD,

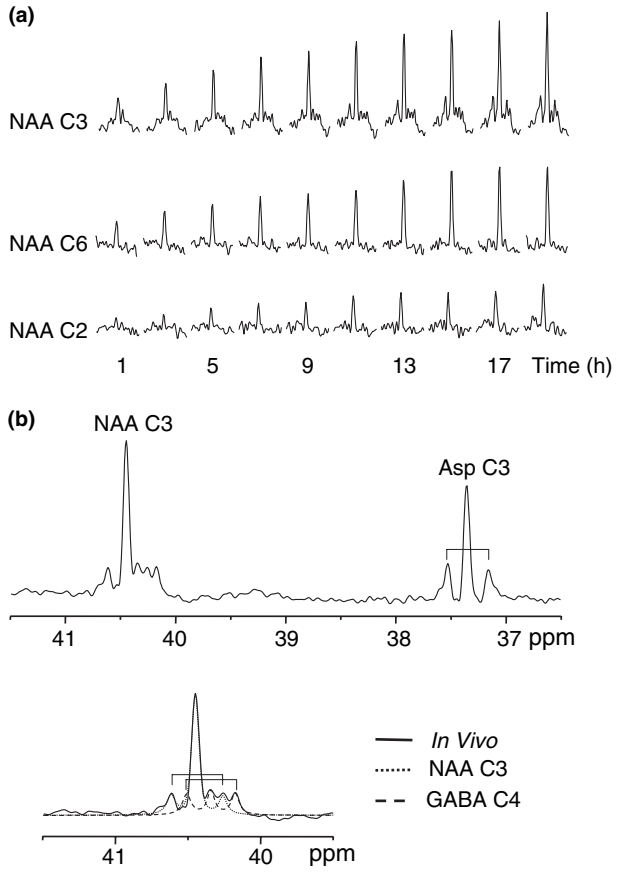

Fig. 2 Detection of progressive label incorporation into all three *N*-acetyl aspartate (NAA) resonances. (a) Horizontal stack plots of NAA C3 (40.5 ppm), NAA C6 (22.8 ppm) and NAA C2 (54.0 ppm) spectra show label incorporation into NAA resonances up to 19 h of [1-^{13}C]glucose infusion (1024 scans each, TR = 1.5 s). Resonance intensities varied because of the radiofrequency excitation profile, which was weaker at the C2 position. (b) The multiple resonances at 40.5 ppm were fitted and found to be consistent with a superposition of multiplets (singlet + doublet) with ^{13}C–^{13}C homonuclear coupling of 34 Hz at the position of NAA C3 (40.5 ppm) as well as that of GABA C4 (40.4 ppm). The brackets indicate the J coupling of 34 Hz. The homonuclear ^{13}C–^{13}C coupling in the aspartyl moiety of NAA (NAA C3) was found to be consistent with the isotopomer of aspartate C3 (upper trace). TR, repetition time.

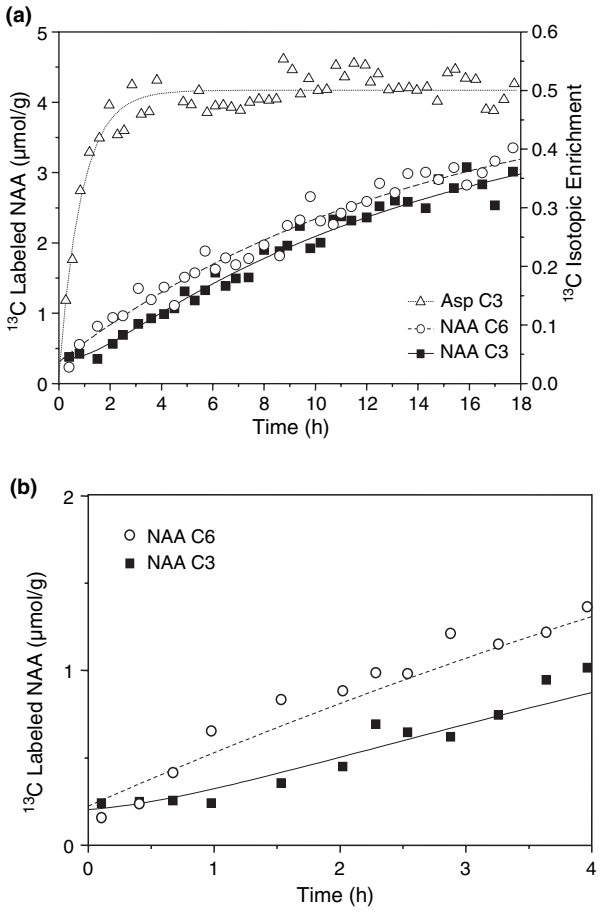

Fig. 3 Time-resolved observation of *N*-acetyl aspartate (NAA) metabolism. (a) The detection of ^{13}C-label incorporation into NAA C3 and C6 during [1-^{13}C]glucose infusion (see left axis). The time course of aspartate C3 (triangles, see right axis) shows initial label delay because of the flux rate of the TCA cycle and label exchanges between intermediary metabolites. The label time constant of aspartate C3, τ_{Asp} = 1 h (dotted line), led to the delayed label incorporation of NAA C3. (b) The initial time course of NAA shows time delay of label incorporation of NAA C3 by ~1.5 h compared to that of NAA C6, consistent with the slower labeling of the precursor of NAA C3, aspartate, compared to the precursor of NAA C6, acetyl-CoA, which was assumed to mimic the labeling of plasma glucose (see Appendix). Shown is the average data from eight animals.

$n = 8$). The time constant of aspartate C3 from the turnover fit (eqn A4), τ_{Asp}, was 1.0 ± 0.2 h (mean ± SD, $n = 8$). For NAA C3, the time course was fitted using a two-exponential fit (Fig. 3) reflecting an exponential input function of aspartate (eqn 2) and the estimated turnover rate of NAA C3 was $V_{NAA} = 0.6 \pm 0.1$ μmol/(g h) with the time constant of NAA C3, $\tau_{NAA3} = 13 \pm 2$ h (mean ± SD, $n = 8$). From the fits, the steady-state ^{13}C concentrations of NAA C6 and C3 were estimated at 4.2 ± 0.2 μmol/g and 3.8 ± 0.2 μmol/g, respectively. The relationship between ^{13}C isotopomers of NAA C3 and aspartate C3 was analyzed using linear regression of the doublet-to-(singlet + doublet) signal ratios of NAA C3 and aspartate C3. Isotopomer analysis of NAA C3 and aspartate C3 showed a linear relationship with a slope of 0.81 ± 0.03 (slope ± fit error, $r = 0.9$, $p = 0.0015$, $n = 8$, data not shown).

^{13}C-label incorporation into the GSH Glu C4 at 32.2 ppm was observed up to 19 h of [1-^{13}C]glucose infusion (Fig. 4a). Vertical stack plots of the averaged spectra with a temporal resolution of 3 h (2048 scans each, TR = 1.5 s) showed substantially slower label incorporation of GSH Glu C4 compared to GABA C2 (35.12 ppm), glutamtate C4

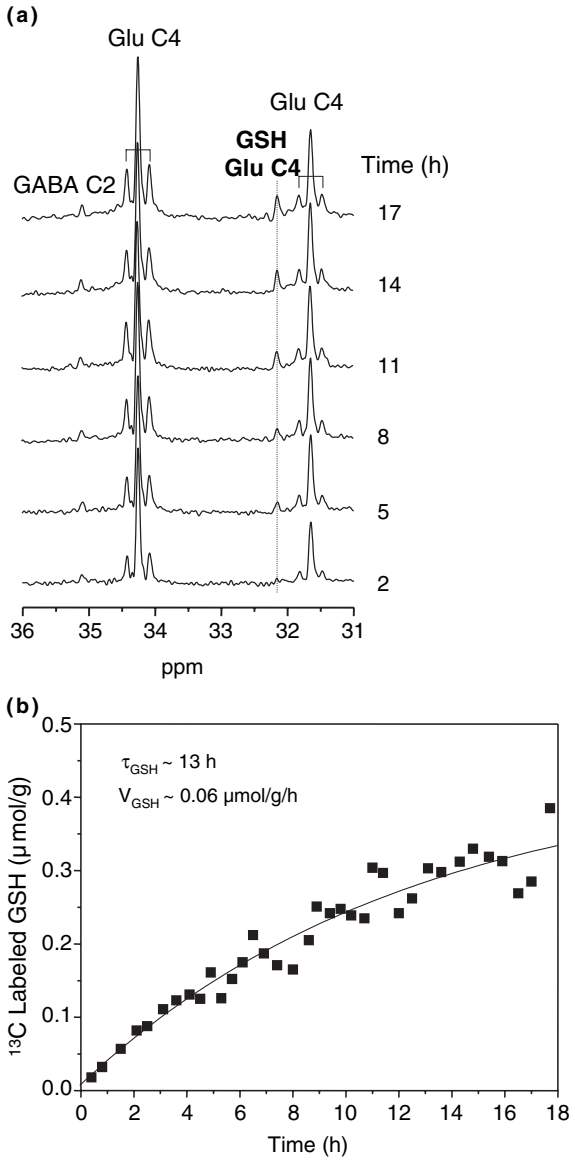

Fig. 4 Time-resolved observation of glutathione (GSH) metabolism *in vivo*. (a) Time course of ^{13}C-label incorporation into GSH Glu C4 (32.2 ppm, vertical dotted line) up to 19 h of [1-^{13}C]glucose infusion. GSH appears very slowly compared to GABA C2 (35.1 ppm), glutamate C4 (Glu C4, 34.27 ppm) and glutamine C4 (Gln C4, 31.7 ppm), which reach steady state much more rapidly. Each spectrum in the stack plot is averaged with a temporal resolution of 3 h (2048 scans each, TR = 1.5 s) and mean values of each time interval are shown in the right axis. The resonance of glutamate C4 at 34.27 ppm was used as a reference for all peak assignments of the spectra. Note that the GSH resonance continues to increase over time, whereas the GABA C2 and Glu C4 resonances are close to constant in time, indicating much faster turnover, consistent with our previous results (Pfeuffer *et al.* 1999). TR, repetition time. (b) The time course of GSH shows a very slow turnover rate of $V_{GSH} \sim 0.06$ µmol/(g h) and time constant of $\tau_{GSH} = 13$ h. Shown is the average of eight animals.

(34.27 ppm) and glutamine C4 (31.66 ppm). The estimated turnover rate of GSH was 0.06 ± 0.02 µmol/(g h) (mean ± SD, $n = 8$) with the time constant of GSH from the turnover fit, $\tau_{GSH} = 13 \pm 2$ h (mean ± SD, $n = 8$). Based on an exponential fit (Fig. 4b), the steady-state ^{13}C concentration of GSH was estimated at 0.4 ± 0.1 µmol/g (mean ± SD, $n = 8$). Assuming that 50% of GSH was labeled by ^{13}C at infinite time (because, at most, half of the acetyl-CoA will be labeled from the [1-^{13}C] glucose used), the estimated total GSH concentration was ~0.8 µmol/g, which is comparable to the cortical GSH concentration in the rat brain (Pfeuffer *et al.* 1999), suggesting complete turnover of the GSH pool in the brain *in vivo*.

Discussion

This study reports the measurement of label incorporation into the acetyl as well as the aspartyl moieties of NAA in three resonances of NAA, i.e. the NAA C2, C3 and C6 (Fig. 2a) in the intact rat brain *in vivo*. In addition, ^{13}C–^{13}C homonuclear coupling of NAA C3 and GABA C4 was discovered. It was interesting to note that approximately 2 h after starting the infusion of [1-^{13}C]glucose, the acetyl (C6) as well as the aspartyl (C2 and C3) signals of NAA clearly increased with time (Fig. 2a). An early study in brain extracts observed labeling of the acetyl moiety of NAA but not that of the aspartyl moiety 2 h after administering label (Kunnecke *et al.* 1993). Their observation is consistent with our study, which showed that label incorporation into the aspartyl moiety was delayed by approximately 1.5–2 h. The question thus arises as to how the amount of label incorporated into the two NAA moieties could differ and be delayed. The data presented in this study suggests that the delayed label incorporation into NAA C3 is a result of the delayed labeling of the precursor of NAA C3, namely aspartate C3, compared to the labeling of the precursor of NAA C6, namely acetyl-CoA C2. As illustrated in Fig. 1, label from glucose labeled in the C1 position will be incorporated into the C2 position of acetyl-CoA, which leads to labeling of NAA C6. It is assumed that the labeling of acetyl-CoA C2 is much faster than that of aspartate C3, because acetyl-CoA is the label precursor of aspartate through the TCA cycle. In addition, in order for label to be incorporated into the aspartyl moiety of NAA (NAA C3), aspartate needs to be labeled first, which happens through transamination of oxaloacetate, a TCA cycle intermediate. As the label enters the TCA cycle from acetyl-CoA, it first labels the C4 of 2-oxoglutarate, which exchanges label with glutamate, whose concentration is approximately 10 µmol/g in the mammalian brain. Recent studies have indicated that this exchange rate is on the order of the rate of the pyruvate dehydrogenase flux (Gruetter *et al.* 2001; Choi *et al.* 2002; Henry *et al.* 2002), and the size of the glutamate pool can significantly affect the labeling of the TCA cycle intermediates (Gruetter *et al.* 2001). Thus, the

label incorporation into the aspartyl moiety of NAA from glucose that involves label scrambling in the TCA cycle and label exchange with amino acid pools (Fig. 1) delays the labeling of aspartate by ~1.5 h (Fig. 3a), whereas ^{13}C-labeled glucose reaches steady state very rapidly (Choi *et al*. 2002). Because the label precursor of the aspartyl moiety of NAA was labeled more slowly than the label precursor of the acetyl moiety of NAA, the labeling of NAA C3 was delayed compared to that of NAA C6, as observed in this study (Fig. 3).

The simultaneous observation of label incorporation into both acetyl and aspartyl groups of NAA can provide insights into metabolic compartmentation and biosynthesis of NAA. First, the current data can be interpreted as NAA synthesis in a single metabolic compartment, as described above. This was further supported by the isotopomer analysis. Second, as the synthesis of NAA has been ascribed to the neuronal mitochondria (Benuck and D'Adamo 1968; Clark 1998), the current data is consistent with the labeling of aspartate representing mainly the neuronal compartment (Gundersen *et al*. 2001). The observation of similar labeling patterns and isotopic enrichment between NAA and aspartate suggests that aspartate is the precursor of NAA and supports the hypothesis that NAA synthesis occurs in the neuronal compartment.

From fitting a mathematical model of NAA metabolism (see Fig. 1 and Appendix), the steady-state concentration of ^{13}C label was calculated in both the aspartyl and acetyl moieties of NAA. The steady-state ^{13}C pool size of NAA was ~4 μmol/g, which indicated complete turnover of NAA when considering that the total concentration of NAA in these regions of the rat brain is approximately 8–9 μmol/g (Pfeuffer *et al*. 1999; Choi and Gruetter 2003) and that ^{13}C label represents maximum 50% of the total concentration of NAA. Complete turnover of NAA requires 2–3 days in the rat brain, as judged from the label time constant of NAA, $\tau_{NAA} = 13–14$ h. Therefore, we conclude that NAA was synthesized very slowly [0.6–0.7 μmol/(g h)] from its precursors, neuronal acetyl-CoA and aspartate, and accounts only for a very small fraction of overall brain glucose metabolism under resting normoxic conditions. In addition, preliminary evidence suggested that NAA concentrations were not affected by extended periods of hypoglycemia (data not shown), further supporting the notion that NAA does not serve as an energy-buffering store in the rat brain.

The turnover rate of GSH was found to be equivalent to that of NAA in the rat brain *in vivo*, but much slower compared to that of other amino acids such as glutamate, glutamine and GABA. Rapid turnover of the GABA pool was indicated, as expected by the early appearance of the C4 and C2 methylene groups of GABA in Fig. 2(a) (top trace) and Fig. 4(a), respectively. The steady-state ^{13}C concentration of GSH was 0.4 μmol/g, which is half of the GSH content in the rat brain *in vivo* measured by ^{1}H NMR spectroscopy (Pfeuffer *et al*. 1999; Tkac *et al*. 2003), as expected for complete turnover from glucose. The GSH turnover in the living intact brain *in vivo* may provide an important parameter in monitoring metabolic alterations of GSH during oxidative stress in aging and neurodegenerative diseases.

Conclusions

In conclusion, labeling from glucose suggests complete turnover of NAA, with the synthesis occurring in a single kinetic compartment. Furthermore, we conclude that NAA is not likely to serve as a significant buffer of acetyl-CoA units for brain energy metabolism at rest. To what extent NAA may provide acetyl-CoA units under conditions of substrate deprivation remains to be determined. It is thus more likely that NAA plays a role in biosynthetic processes that remain to be identified.

Acknowledgements

This work was supported by NIH grants R01NS38672 (RG), R21DK58004 (RG), R01NS42005 (RG), 8R01EB00315 (IYC) and R03AG022193 (IYC). The 9.4 T magnet was funded in part by a gift from the W. M. Keck Foundation, and the Center for Magnetic Resonance Research is supported in part by a center grant from the BTRP program of NCRR (P41RR08079).

References

Adriany G. and Gruetter R. (1997) A half volume coil for efficient proton decoupling in humans at 4 Tesla. *J. Magn. Reson.* **125**, 178–184.

Bachelard H. and Badar-Goffer R. (1993) NMR spectroscopy in neurochemistry. *J. Neurochem.* **61**, 412–429.

Bains J. S. and Shaw C. A. (1997) Neurodegenerative disorders in humans: the role of glutathione in oxidative stress-mediated neuronal death. *Brain Res. Brain Res. Rev.* **25**, 335–358.

Baslow M. H. (2000) Functions of *N*-acetyl-L-aspartate and *N*-acetyl-L-aspartylglutamate in the vertebrate brain: role in glial cell-specific signaling. *J. Neurochem.* **75**, 453–459.

Baslow M. H. (2003) *N*-Acetylaspartate in the vertebrate brain: metabolism and function. *Neurochem. Res.* **28**, 941–953.

Benuck M. and D'Adamo A. F. Jr (1968) Acetyl transport mechanisms. Metabolism of *N*-acetyl-L-aspartic acid in the non-nervous tissues of the rat. *Biochim. Biophys. Acta* **152**, 611–618.

Benzi G., Pastoris O., Marzatico F. and Villa R. F. (1988) Influence of aging and drug treatment on the cerebral glutathione system. *Neurobiol. Aging* **9**, 371–375.

Blakely R. D. and Coyle J. T. (1988) The neurobiology of *N*-acetylaspartylglutamate. *Int. Rev. Neurobiol.* **30**, 39–100.

Brown F. F., Campbell I. D., Kuchel P. W. and Rabenstein D. C. (1977) Human erythrocyte metabolism studies by 1H spin echo NMR. *FEBS Lett.* **82**, 12–16.

Cerdan S., Kunnecke B. and Seelig J. (1990) Cerebral metabolism of [1,2–13C2]acetate as detected by in vivo and in vitro 13C NMR. *J. Biol. Chem.* **265**, 12916–12926.

Chang M. L., Klaidman L. K. and Adams J. D. Jr (1997) The effects of oxidative stress on in vivo brain GSH turnover in young and mature mice. *Mol. Chem. Neuropathol.* **30**, 187–197.

Choi I.-Y. and Gruetter R. (2000) Dynamic detection of *N*-Acetyl-Aspartate and Glutathione turnover using in vivo 13C NMR. *J. Neurochem.* **74**, S86A.

Choi I. Y. and Gruetter R. (2003) In vivo 13C NMR assessment of brain glycogen concentration and turnover in the awake rat. *Neurochem. Int.* **43**, 317–322.

Choi I.-Y., Tkac I., Ugurbil K. and Gruetter R. (1999) Noninvasive measurements of [1–13C] glycogen concentrations and metabolism in rat brain in vivo. *J. Neurochem.* **73**, 1300–1308.

Choi I.-Y., Tkac I. and Gruetter R. (2000) Single-shot, three-dimensional 'non-echo' localization method for in vivo NMR spectroscopy. *Magn. Reson. Med.* **44**, 387–394.

Choi I.-Y., Lee S.-P., Kim S.-G. and Gruetter R. (2001) In vivo measurements of brain glucose transport using the reversible Michaelis–Menten model and simultaneous measurements of cerebral blood flow changes during hypoglycemia. *J. Cereb. Blood Flow Metab.* **21**, 653–663.

Choi I. Y., Lei H. and Gruetter R. (2002) Effect of deep pentobarbital anesthesia on neurotransmitter metabolism in vivo: on the correlation of total glucose consumption with glutamatergic action. *J. Cereb. Blood Flow Metab.* **22**, 1343–1351.

Choi I. Y., Seaquist E. R. and Gruetter R. (2003) Effect of hypoglycemia on brain glycogen metabolism in vivo. *J. Neurosci. Res.* **72**, 25–32.

Clark J. B. (1998) *N*-Acetyl aspartate: a marker for neuronal loss or mitochondrial dysfunction. *Dev. Neurosci.* **20**, 271–276.

Clarke D. D., Greenfield S., Dicker E., Tirri L. J. and Ronan E. J. (1975) A relationship of *N*-acetylaspartate biosynthesis to neuronal protein synthesis. *J. Neurochem.* **24**, 479–485.

Cohen S. M. (1987) 13C and 31P NMR study of gluconeogenesis: utilization of 13C-labeled substrates by perfused liver from streptozotocin-diabetic and untreated rats. *Biochemistry* **26**, 563–572.

Coyle J. T. and Puttfarcken P. (1993) Oxidative stress, glutamate, and neurodegenerative disorders. *Science* **262**, 689–695.

D'Adamo A. F. Jr and Yatsu F. M. (1966) Acetate metabolism in the nervous system. *N*-Acetyl-L-aspartic acid and the biosynthesis of brain lipids. *J. Neurochem.* **13**, 961–965.

D'Adamo A. F. Jr, Gidez L. I. and Yatsu F. M. (1968) Acetyl transport mechanisms. Involvement of *N*-acetyl aspartic acid in de novo fatty acid biosynthesis in the developing rat brain. *Exp. Brain Res.* **5**, 267–273.

Dringen R., Verleysdonk S., Hamprecht B., Willker W., Leibfritz D. and Brand A. (1998) Metabolism of glycine in primary astroglial cells: synthesis of creatine, serine, and glutathione. *J. Neurochem.* **70**, 835–840.

Dringen R., Kussmaul L., Gutterer J. M., Hirrlinger J. and Hamprecht B. (1999) The glutathione system of peroxide detoxification is less efficient in neurons than in astroglial cells. *J. Neurochem.* **72**, 2523–2530.

Farnsworth P. N. and Schleich T. (1985) Progress toward the establishment of nuclear magnetic resonance measurements as an index of in vivo lens functional integrity. *Curr. Eye Res.* **4**, 291–297.

Gruetter R. (1993) Automatic, localized in vivo adjustment of all first- and second-order shim coils. *Magn. Reson. Med.* **29**, 804–811.

Gruetter R. (2002) In vivo 13C NMR studies of compartmentalized cerebral carbohydrate metabolism. *Neurochem. Int.* **41**, 143–154.

Gruetter R. (2004) Principles of the measurement of neuro-glial metabolism using in vivo 13C NMR spectroscopy, in *Advances in Molecular and Cell Biology*, Vol. 31 (Hertz L., ed.), pp. 409–433. Elsevier, Amsterdam.

Gruetter R., Seaquist E., Kim S.-W. and Ugurbil K. (1998a) Localized *in vivo* ^{13}C NMR of glutamate metabolism. Initial results at 4 Tesla. *Dev. Neurosci.* **20**, 380–388.

Gruetter R., Weisdorf S. A., Rajanayagan V., Terpstra M., Merkle H., Truwit C. L., Garwood M., Nyberg S. L. and Ugurbil K. (1998b) Resolution improvements in in vivo 1H NMR spectra with increased magnetic field strength. *J. Magn. Reson.* **135**, 260–264.

Gruetter R., Seaquist E. R. and Ugurbil K. (2001) A mathematical model of compartmentalized neurotransmitter metabolism in the human brain. *Am. J. Physiol. Endocrinol. Metab.* **281**, E100–E112.

Gundersen V., Fonnum F., Ottersen O. P. and Storm-Mathisen J. (2001) Redistribution of neuroactive amino acids in hippocampus and striatum during hypoglycemia: a quantitative immunogold study. *J. Cereb. Blood Flow Metab.* **21**, 41–51.

Guo N., McIntosh C. and Shaw C. (1992) Glutathione: new candidate neuropeptide in the central nervous system. *Neuroscience* **51**, 835–842.

Henry P.-G., Lebon V., Vaufrey F., Brouillet E., Hantraye P. and Bloch G. (2002) Decreased TCA cycle rate in the rat brain after acute 3-NP treatment measured by in vivo 1H-{13C} NMR spectroscopy. *J. Neurochem.* **82**, 857–866.

Henry P. G., Oz G., Provencher S. and Gruetter R. (2003) Toward dynamic isotopomer analysis in the rat brain in vivo: automatic quantitation of 13C NMR spectra using LCModel. *NMR Biomed.* **16**, 400–412.

Hyder F., Chase J. R., Behar K. L., Mason G. F., Siddeek M., Rothman D. L. and Shulman R. G. (1996) Increased tricarboxylic acid cycle flux in rat brain during forepaw stimulation detected with 1H [13C] NMR. *Proc. Natl Acad. Sci. USA* **93**, 7612–7617.

Jacobson K. B. (1959) Studies on the role of *N*-acetylaspartic acid in mammalian brain. *J. Gen. Physiol.* **43**, 323–333.

Jans A. W. and Leibfritz D. (1988) A 13C-NMR study on the influxes into the tricarboxylic acid cycle of a renal epithelial cell line, LLC-PK1/Cl4: the metabolism of [2–13C]glycine, L-[3–13C]alanine and L-[3–13C]aspartic acid in renal epithelial cells. *Biochim. Biophys. Acta* **970**, 241–250.

Ketterer B. (1988) Protective role of glutathione and glutathione transferases in mutagenesis and carcinogenesis. *Mutat. Res.* **202**, 343–361.

Kuchel P. W. and Chapman B. E. (1983) Proton NMR studies of creatine in human erythrocytes. *Biomed. Biochim. Acta* **42**, 1143–1149.

Kunnecke B., Cerdan S. and Seelig J. (1993) Cerebral metabolism of [1,2–13C2]glucose and [U-13C4]3-hydroxybutyrate in rat brain as detected by 13C NMR spectroscopy. *NMR Biomedicine* **6**, 264–277.

Lang C. A., Naryshkin S., Schneider D. L., Mills B. J. and Lindeman R. D. (1992) Low blood glutathione levels in healthy aging adults. *J. Lab. Clin. Med.* **120**, 720–725.

Margolis R. V., Barkulis S. S. and Geiger A. (1960) A comparison between the incorporation of 14C from glucose into *N*-acetyl-L-aspartic acid and aspartic acid in brain perfusion experiments. *J. Neurochem.* **5**, 379–382.

Mason G. F., Rothman D. L., Behar K. L. and Shulman R. G. (1992) NMR determination of the TCA cycle rate and alpha-ketoglutarate/glutamate exchange rate in rat brain. *J. Cereb. Blood Flow Metab.* **12**, 434–447.

Meyerhoff D. J., MacKay S., Bachman L., Poole N., Dillon W. P., Weiner M. W. and Fein G. (1993) Reduced brain *N*-acetylaspartate suggests neuronal loss in cognitively impaired human immunodeficiency virus-seropositive individuals: in vivo 1H magnetic resonance spectroscopic imaging. *Neurology* **43**, 509–515.

Moreno A., Ross B. D. and Bluml S. (2001) Direct determination of the *N*-acetyl-L-aspartate synthesis rate in the human brain by 13C MRS and [1–13C]glucose infusion. *J. Neurochem.* **77**, 347–350.

Nadler J. V. and Cooper J. R. (1972) Metabolism of the aspartyl moiety of *N*-acetyl-L-aspartic acid in the rat brain. *J. Neurochem.* **19**, 2091–2105.

O'Neal R. M., Koeppe R. E. and Williams E. I. (1966) Utilization in vivo of glucose and volatile fatty acids by sheep brain for the synthesis of acidic amino acids. *Biochem. J.* **101**, 591–597.

Ogita K., Enomoto R., Nakahara F., Ishitsubo N. and Yoneda Y. (1995) A possible role of glutathione as an endogenous agonist at the *N*-methyl-D-aspartate recognition domain in rat brain. *J. Neurochem.* **64**, 1088–1096.

Pfeuffer J., Tkac I., Provencher S. W. and Gruetter R. (1999) Toward an in vivo neurochemical profile: Quantification of 18 metabolites in short-echo-time 1H NMR spectra of the rat brain. *J. Magn. Reson.* **141**, 104–120.

Rothman D. L., Sibson N. R., Hyder F., Shen J., Behar K. L. and Shulman R. G. (1999) In vivo nuclear magnetic resonance spectroscopy studies of the relationship between the glutamate–glutamine neurotransmitter cycle and functional neuroenergetics. *Philos. Trans. R. Soc. Lond. B Biol. Sci.* **354**, 1165–1177.

Shaw C. A., Pasqualotto B. A. and Curry K. (1996) Glutathione-induced sodium currents in neocortex. *Neuroreport* **7**, 1149–1152.

Skibsted U. and Hansen P. E. (1990) 1H NMR spin-echo spectroscopy of human erythrocytes. Transformation of exogenous compounds. *NMR Biomed.* **3**, 248–258.

Tallan H. H. (1957) Studies on the distribution of *N*-Acetyl-L-Aspartic acid in brain. *J. Biol. Chem.* **224**, 41–45.

Taylor D. L., Davies S. E., Obrenovitch T. P., Doheny M. H., Patsalos P. N., Clark J. B. and Symon L. (1995) Investigation into the role of *N*-acetylaspartate in cerebral osmoregulation. *J. Neurochem.* **65**, 275–281.

Tkac I., Rao R., Georgieff M. K. and Gruetter R. (2003) Developmental and regional changes in the neurochemical profile of the rat brain determined by in vivo 1H NMR spectroscopy. *Magn. Reson. Med.* **50**, 24–32.

Tyson R. L. and Sutherland G. R. (1998) Labeling of *N*-acetylaspartate and *N*-acetylaspartylglutamate in rat neocortex, hippocampus and cerebellum from [1–13C]glucose. *Neurosci. Lett.* **251**, 181–184.

Varga V., Jenei Z., Janaky R., Saransaari P. and Oja S. S. (1997) Glutathione is an endogenous ligand of rat brain *N*-methyl-D-aspartate (NMDA) and 2-amino-3-hydroxy-5-methyl-4-isoxazolepropionate (AMPA) receptors. *Neurochem. Res.* **22**, 1165–1171.

Appendix

Mathematical model of *N*-acetyl aspartate metabolism

The scheme in Fig. 1 was used to model the rate of ^{13}C-label incorporation into NAA C3 and C6. In this metabolic model, steady state was assumed, i.e. the concentration and the metabolic rates of NAA were assumed to be constant in time. It was further assumed that the isotopic enrichment of acetyl-CoA was raised to a steady-state value very rapidly compared to the rate of NAA turnover. This assumption was justified by the rapid rise in the isotopic enrichment of plasma glucose.

Using mathematical formulations intrinsic to tracer (or labeling) studies (Mason *et al*. 1992; Gruetter *et al*. 1998a), the metabolic modeling of the rate of ^{13}C-label incorporation into NAA C6, $^{13}NAA_6$, can be expressed as a differential equation,

$$\frac{d^{13}NAA_6}{dt} = V_{NAA}^{(in)} \frac{^{13}\text{Acetyl-CoA}_2}{\text{Acetyl-CoA}} - V_{NAA}^{(out)} \frac{^{13}NAA_6(t)}{NAA} \quad \text{(A1)}$$

where ^{13}Acetyl-CoA$_2$/Acetyl-CoA is the isotopic enrichment of acetyl-CoA (assumed to be 0.5 times that of glucose) and NAA is the total concentration of NAA. $V_{NAA}^{(in)}$ is the synthesis rate of NAA and $V_{NAA}^{(out)}$ is the degradation rate of NAA. At steady state no net synthesis of NAA occurs by definition, hence $V_{NAA}^{(in)} = V_{NAA}^{(out)} = V_{NAA}$.

With negligible concentration changes of NAA as evidenced by ^{1}H NMR spectroscopy, synthesis and degradation rates of NAA are the same and equal to V_{NAA}. The solution of eqn A1 is

$$\frac{^{13}NAA_6(t)}{NAA} = A + Be^{(\frac{-t}{\tau_{NAA}})} \quad \text{(A2)}$$

where $\tau_{NAA} = NAA/V_{NAA}$, and A and B are the constants determined by the initial and final conditions, i.e. $^{13}NAA_6(t = 0) = 0.011$ NAA and $^{13}NAA_6(t = \infty) = 0.5$ NAA, which are 1.1% natural abundance of ^{13}C label before infusion of ^{13}C-enriched glucose (t = 0) and 50% of ^{13}C label at infinite time ($t = \infty$), respectively, which leads to eqn 1.

Unlike the labeling of acetyl-CoA, that of aspartate does not reach steady state immediately, instead it is delayed because of label exchange between intermediary metabolites in the mitochondrion and the cytosolic amino acids. The calculation that follows demonstrates that delayed labeling of aspartate C2 and C3 results in further delayed labeling of NAA C2 and C3 that can be explicitly expressed in mathematical terms. The metabolic modeling of the rate of label incorporation into NAA C3 (the same for NAA C2) can be expressed as

$$\frac{d^{13}NAA_3}{dt} = V_{NAA} \frac{^{13}Asp_3(t)}{Asp} - V_{NAA} \frac{^{13}NAA_3(t)}{NAA} \quad \text{(A3)}$$

where $^{13}Asp_3$ is the ^{13}C concentration of aspartate C3 and Asp is the total concentration of aspartate.

The rate of ^{13}C-label incorporation into the C3 of aspartate can be modeled in a similar manner as $^{13}NAA_6$ in eqn A2 as

$$\frac{^{13}Asp_3(t)}{Asp} = C + De^{(\frac{-t}{\tau_{Asp}})} \quad \text{(A4)}$$

where in our experiments, C = 0.5 and D = − 0.489.

A trial solution for eqn A3 can be expressed as

$$\frac{^{13}NAA_3(t)}{NAA} = E + Fe^{(\frac{-t}{\tau_{NAA}})} + Ge^{(\frac{-t}{\tau_{Asp}})} \quad \text{(A5)}$$

Taking the derivative of eqn A5 and equating it with eqn A3 yields the following relationships:

$$\tau_{NAA} = NAA/V_{NAA}, \quad \text{(A6)}$$

$$E = C = 0.5, \quad \text{(A7)}$$

$$G = -D\frac{\tau_{Asp}}{\tau_{NAA} - \tau_{Asp}} = 0.489\frac{\tau_{Asp}}{\tau_{NAA} - \tau_{Asp}} \quad \text{(A8)}$$

Constant F is determined by the initial condition of $^{13}NAA_3$ ($t = 0$) = 0.011 NAA and eqns A7 and A8, which leads to eqn 2.

A slower initial rate of label incorporation into NAA C3 compared to that into NAA C6 can be explained by the presence of the last term in eqn 2, which has a positive coefficient because $\tau_{NAA} > \tau_{Asp}$. If the aspartate pool turns over very fast ($\tau_{Asp} \sim 0$), eqn 2 will be equivalent to eqn 1 with no time lag in the labeling of NAA C3.

